Current distribution and local power dissipation in the two-component deterministic percolation model

1993 J. Phys. A: Math. Gen. 26 4223

(http://iopscience.iop.org/0305-4470/26/17/029)

J. Phys. A: Math. Gen. 26 (1993) 4223–4235. Printed in the UK

Current distribution and local power dissipation in the two-component deterministic percolation model

K W Yu and P Y Tong

Department of Physics, The Chinese University of Hong Kong, Shatin, New Territories, Hong Kong

Received 24 September 1992, in final form 29 March 1993

Abstract. We have investigated the current distribution and local power dissipation in the two-component deterministic percolation model in which the ratio of conductance h is regarded as a small parameter. The iterative nature of the model enables us to find exact recursion relations for the current distribution. For an extremely small h such that $hL^{\phi} \ll 1$, where L is the size of the lattice and ϕ the crossover exponent, we find that $D(\alpha) \approx \exp(-A[\alpha - B(\log L)^2]/(\log L)^3)$, where $D(\alpha)\,d\alpha$ is the number of currents with $\alpha < -\log I_i < \alpha + d\alpha$; I_i is the current in bond i and A, B are constants. The current distribution is well approximated by a Gaussian with the mean varying with the size as $(\log L)^2$ while the variance as $(\log L)^3$. As a result, both the most probable current and the minimum current scale with L as exp[−constant $(\log L)^2$]. Similar results are obtained for the distribution of local power dissipation.

1. Introduction

The study of current distribution in the random resistor network (RRN) near the percolation threshold has recently received interest as it reveals very rich structures [1, 2] common in many disordered systems near a critical point. Recently, similar studies have been extended to the two-component RRN, in which the effect of the non-zero conductance of insulating bonds is taken into account [3–6]. To be more precise, we consider a two-dimensional lattice (the generalization to arbitrary dimensions is straightforward) and we associate with each bond a conductance σ_g with probability p and σ_p with probability 1-p where σ_g is the conductance of good conducting bonds while σ_p is that of the poor conducting bonds and $\sigma_g > \sigma_p$. The conductance ratio $h = \sigma_p/\sigma_g$ governs the crossover from the fractal ($h = 0$) to homogeneous ($h = 1$) behaviours.

It has been found that all positive multifractal moments of current scale with a *single* crossover exponent [3–5]. However, the scaling of negative moments has not been studied. The negative moment of the current distribution is dominated by the minimum current, which is in general very difficult to determine accurately in numerical simulation. By employing a new method, we have succeeded in obtaining the minimum current in the two-component RRN [6]. The minimum current is found to scale anomalously with the conductance ratio h as $I_{\min}(h) \approx \exp[-\text{constant}\,(\log h)^2]$. The exponential behaviour indicates that the minimum current falls off faster than any power law. In fact such an anomalous scaling behaviour is quite similar to that in

0305-4470/93/174223+13 $07.50

diffusion-limited aggregations [7]. The minimum growth-site probability scales with system size as $\exp[-A(\log L)^2]$. This leads to the failure of conventional multifractal analysis [8–9] as the negative moments do not scale with system size as a power law [7]. In view of this, we shall use an alternative approach to analyse the problem.

The organization of the paper is as follows. We investigate the current distribution of the two-component deterministic percolation model (DPM), the construction of which will be described in the next section. We briefly discuss the renormalization group transformation of the network conductance. In section 3, we study the scaling and crossover behaviours of the minimum current. In section 4, we derive the recursion relations for the current distribution and obtain an analytic solution by using the generating function technique [10]. The distribution is well approximated by a Gaussian with its mean varying as $\exp[-A(\log L)^2]$ and variance goes as $(\log L)^3$. In sections 5, we perform similar studies for the distribution of local power dissipation. We shall discuss the generality of the results and suggest numerical simulation be done to check the analytical results. The possibility of comparison with experiment will also be discussed.

2. The determinstic percolation model (DPM)

The deterministic percolation model (DPM) is an extension of the fractal lattice, originally proposed by Kirkpatrick [11] to model the percolation backbone. Here we follow Clerc *et al* [6, 12] to extend the constructions to the two-component case. Starting with a filled square, one divides it into four equal squares and replaces the upper right quadrant by an empty square to obtain the first generation. The lateral size is increased by a factor of two. The second generation is obtained from the first generation by replacing each square by two types of generators. The generator for a filled square is exactly the same as the first generation but the generator for an empty square is complementary to that of the filled square, i.e. the upper right quadrant is filled while the rest are empty. The process is repeated *ad infinitum* to obtain the deterministic lattice.

An equivalent circuit model [6, 12] is shown in figure 1(*a*) in that the good conducting bond at the right is a parallel combination of $(4f-2)$ good conductors while that at the left has $4(1-f)$ poor conductors, where f is a filling factor and $\frac{1}{2}<f<1$. Similar notations are used in figure 1(*b*) to model the poor conducting bonds. Starting with a finite deterministic lattice at the nth generation, we can use a renormalization group (RG) method to obtain the renormalized conductance of the $(n-1)$th generation (i.e. first level of renormalization). From figures 1(*a*) and (*b*), the impedance of the good conductor X_k and that of the poor conductor Y_k at the kth level of renormalization are related to those of the $(k-1)$th level of renormalization by the following recursion relations [6, 12]

$$X_k=\frac{1}{2}X_{k-1}+\frac{X_{k-1}Y_{k-1}}{4(1-f)X_{k-1}+(4f-2)Y_{k-1}} \tag{1a}$$

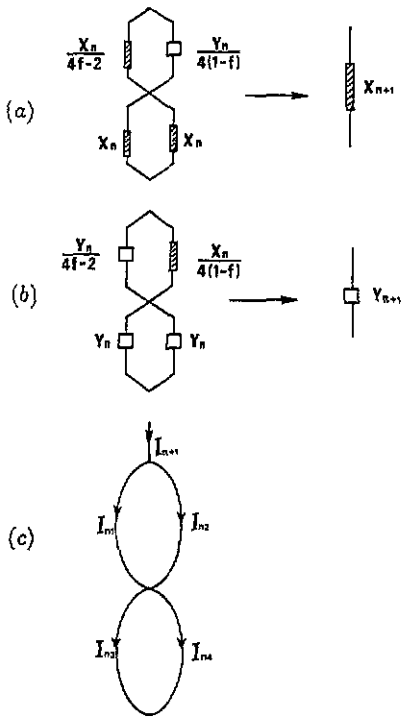

Figure 1. The renormalization process of the two-component deterministic percolation model: (*a*) good conductor→good conductor, (*b*) poor conductor→poor conductor, (*c*) the four currents in a typical element.

$$Y_k=\frac{1}{2}Y_{k-1}+\frac{Y_{k-1}X_{k-1}}{4(1-f)Y_{k-1}+(4f-2)X_{k-1}}. \tag{1b}$$

If we denote $h_k=X_k/Y_k$, we arrive at a recursion relation for h_k

$$h_k=S(h_{k-1}) \tag{2}$$

where $S(h)$ is a one-parameter iterated map [6, 12]

$$S(h)=h\frac{[(1-f)h+f][(2f-1)h+2(1-f)]}{[fh+(1-f)][2(1-f)h+(2f-1)]}. \tag{3}$$

One can easily show that $h=1$ is a stable fixed point while $h=0$ is an unstable fixed point of the map $S(h)$ [6, 12]. The multipliers associated with the fixed points at $h=1$ and $h=0$ are given by $\lambda_1=2f-1$ and $\lambda_0=2f/(2f-1)$ respectively. Physically, the unstable fixed point at $h=0$ corresponds to the interesting cases of the random resistor network limit in which the poor conductor has no finite conductance, and the random superconducting network limit in which the good conductor has an infinite conductance. We are interested in the scaling region with a small but finite initial value h_0 (in the vicinity of the $h=0$ unstable fixed point) in a finite network so that the subsequent flow to the $h=1$ fixed point leads to a crossover from fractal to homogeneous

behaviour [6].

For convenience of subsequent studies, we define a function $\varphi(h)$ [6, 12] such that

$$\varphi(h)=\frac{(1-f)h+f}{2(1-f)h+(2f-1)}. \tag{4}$$

3. The minimum current

In this section, we obtain the complete set of currents by using elementary circuit analysis. Let I_k be the current at the kth level of renormalization. From figure 1(c), the four currents in the good conductor are given by

$$I_{k1}=(4f-2)(\varphi(h_k)-\tfrac{1}{2})I_{k+1} \tag{5a}$$

$$I_{k2}=4(1-f)h_k(\varphi(h_k)-\tfrac{1}{2})I_{k+1} \tag{5b}$$

$$I_{k3}=I_{k4}=\tfrac{1}{2}I_{k+1}. \tag{5c}$$

Similarly, the four currents in the poor conductor are given by

$$I_{k1}=(4f-2)(\varphi(h_k)h_k/h_{k+1}-\tfrac{1}{2})I_{k+1} \tag{6a}$$

$$I_{k2}=4(1-f)h_k^{-1}(\varphi(h_k)h_k/h_{k+1}-\tfrac{1}{2})I_{k+1} \tag{6b}$$

$$I_{k3}=I_{k4}=\tfrac{1}{2}I_{k+1}. \tag{6c}$$

The maximum current is located at the first bond of the good conductors while the minimum current of the network is located at the first bond of the poor conductors (see figure 1) at any generation. A more comprehensive study of the minimum current can be found in [6]. Here we briefly summarize the result and interested readers are referred to [6]. The minimum current is given by [6]

$$\frac{I_{\min}^{(n+1)}(h_0)}{I_{\min}^{(n+1)}(1)}=\exp(-(\ln h_0)^2/2\ln\lambda_0)H(\lambda_0^n h_0) \tag{7}$$

where $\lambda_0=2f/(2f-1)$ is the multiplier associated with the unstable fixed point at $h=0$. In figure 2, we plot the normalized minimum current $I_{\min}^{(n+1)}(h_0)/I_{\min}^{(n+1)}(1)$ as a function of h_0L^{ϕ} in a log–log plot, we can see that as n increases the curve crosses over from a rapidly decreasing region towards a constant. The crossover occurs clearly at $n\approx n^*(h_0)\approx-\ln h_0/\ln\lambda_0$. In figure 3, we plot the rescaled minimum current $(I_{\min}^{(n+1)}(h_0)/I_{\min}^{(n+1)}(1))\exp(-(\ln h_0)^2/2\ln\lambda_0)$ against h_0L^{ϕ}, The collapse of all data on a universal curve is evident.

4. Recursion relations for the current distribution

In the preceding section, we discussed the scaling and crossover behaviours of the minimum current only. In this section, we shall focus on the size and conductance ratio dependence of the current distribution. We derive the recursion relations and obtain analytic solutions for the current distribution in the deterministic percolation model.

At the kth level of renormalization, the lattice has a size 2^{n-k}. Let us define the current distribution at the kth level of renormalization $D_k(\alpha)\,d\alpha$ as the number of

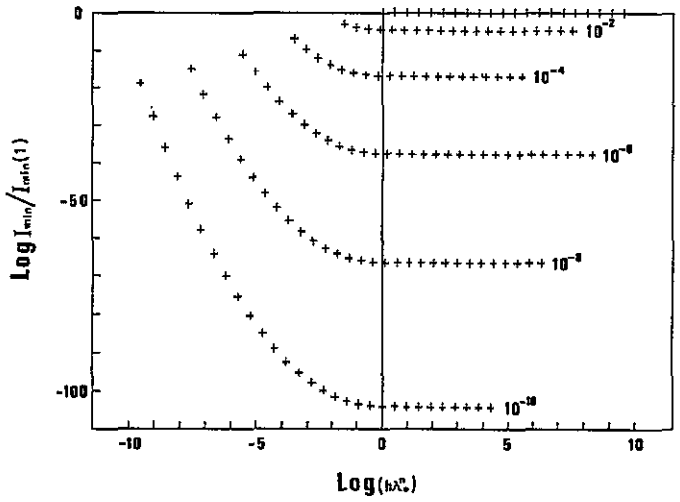

Figure 2. Log–log plot of the normalized minimum current $I_{min}(h_0)/I_{min}(1)$ as a function of $h_0 L^{\phi}$ for $h_0 = 1, 10^{-2}, 10^{-4}$ with n from 1 to 20 and for $h_0 = 10^{-6}, 10^{-8}, 10^{-10}$ with n from 1 to 30. The filling factor is $f = \frac{3}{4}$.

bonds carrying current with $\alpha < \alpha_i < \alpha + d\alpha$ and $\alpha_i = -\log I_i$. For convenience of establishing recursion relations, we also denote $D_k^g(\alpha)$ as the current distribution of the good conductors and $D_k^p(\alpha)$ that of the poor conductors so that $D_k(\alpha) = D_k^g(\alpha) + D_k^p(\alpha)$. The recursion relation for $D_k^f(\alpha)$ and $D_k^p(\alpha)$ can be obtained from (5) and (6) directly. As we are interested in percolating configurations only, the initial conditions at the nth level of renormalization ($k = n$) are $D_n^g(\alpha) = \delta_{\alpha,0}$ and $D_n^p(\alpha) = 0$.

First, we consider the limit of large h_0 so that $\lambda_0^n h_0 \gg 1$ and hence $h_n \approx 1$, the problem reduces to the trivial case of a one-component lattice. The current I_k is just one half of I_{k+1} from (5) and (6). Upon iterating the currents from the nth level of renormalization (i.e. as k decreases), the width of the distribution remains narrow

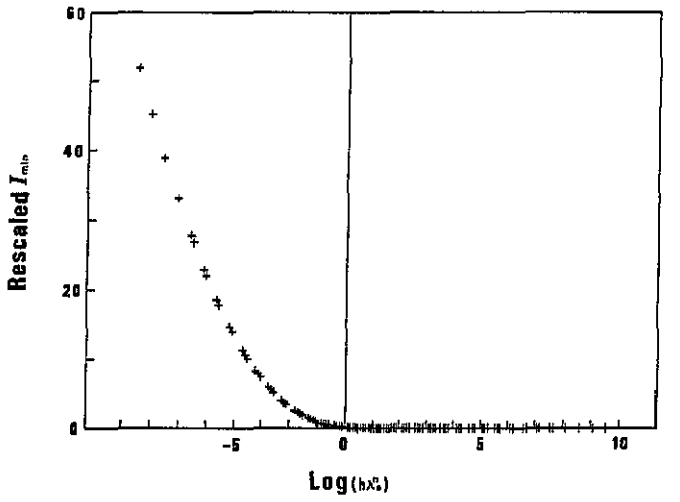

Figure 3. The rescaled minimum current plotted against $h_0 L^{\phi}$ to show perfect data collapse. Same data is used as in figure 2.

until the number of iteration $(n-k)$ reaches a typical value $(n-n^*)$ where $n^* \approx -\log h_0/\log \lambda_0$. For $(n-k)>(n-n^*)$, the iteration of currents begins to broaden the distribution. Without loss of generality, we therefore consider the opposite limit $h_n \approx \lambda_0^n h_0 \ll 1$ and hence $\varphi(h_k) \approx \varphi(0)$. In this limit, the following expressions are asymptotically valid for $0 \leqslant k \leqslant n-1$. For $f=\frac{3}{4}$ and in the good conducting bonds

$$I_{k1} = (\varphi(0) - \tfrac{1}{2}) I_{k+1} \tag{8a}$$

$$I_{k2} = h_k I_{k+1} \tag{8b}$$

$$I_{k3} = I_{k4} = \tfrac{1}{2} I_{k+1} \tag{8c}$$

while in the poor conducting bonds

$$I_{k1} = h_k I_{k+1} \tag{9a}$$

$$I_{k2} = (\varphi(0) - \tfrac{1}{2}) I_{k+1} \tag{9b}$$

$$I_{k3} = I_{k4} = \tfrac{1}{2} I_{k+1}. \tag{9c}$$

We take the logarithm of (8) and let $\alpha = -\log I_k$ and $\alpha' = -\log I_{k+1}$, α' being the pre-image of α. In this way, we obtain from the pre-images the contribution of current distribution at the kth level of renormalization. The recursion relation for the distribution functions are as follows (valid for $0 \leqslant k \leqslant n-1$).

$$\mathsf{D}_k^g(\alpha) = \mathsf{D}_{k+1}^g(\alpha) + 2\mathsf{D}_{k+1}^g(\alpha - \log 2) + \mathsf{D}_{k+1}^p(\alpha) \tag{10a}$$

$$\mathsf{D}_k^p(\alpha) = \mathsf{D}_{k+1}^p(\alpha + k\log\lambda_0 - |\log h_0|) + 2\mathsf{D}_{k+1}^g(\alpha - \log 2) + \mathsf{D}_{k+1}^g(\alpha + k\log\lambda_0 - |\log h_0|). \tag{10b}$$

with initial conditions $\mathsf{D}_n^g(\alpha) = \delta_{\alpha,0}$ and $\mathsf{D}_n^p(\alpha) = 0$. Let us define the Laplace transform for the distribution functions

$$g_m(s) = \int_0^\infty \mathsf{D}_{n-m}^g(\alpha)\, \mathrm{e}^{-s\alpha}\, \mathrm{d}\alpha \tag{11a}$$

$$p_m(s) = \int_0^\infty \mathsf{D}_{n-m}^p(\alpha)\, \mathrm{e}^{-s\alpha}\, \mathrm{d}\alpha \tag{11b}$$

at the mth generation with initial conditions $g_0(s)=1$ and $p_0(s)=0$ at the zeroth generation $(m=0)$. We obtain the recursion relations for $g_m(s)$ and $p_m(s)$:

$$g_m(s) = (1 + 2\,\mathrm{e}^{-s\alpha_2}) g_{m-1}(s) + p_{m-1}(s) \tag{12a}$$

$$p_m(s) = \mathrm{e}^{-s\alpha_1(n-m)} g_{m-1}(s) + (2\,\mathrm{e}^{-s\alpha_2} + \mathrm{e}^{-s\alpha_1(n-m)}) p_{m-1}(s) \tag{12b}$$

where

$$\alpha_1(k) = \alpha_1 - k\log\lambda_0 \tag{13a}$$

$$\alpha_1 = |\log h_0| \tag{13b}$$

$$\alpha_2 = \log 2. \tag{13c}$$

Note that $\alpha_1(n-m)$ is not a constant coefficient while α_2 and α_3 are independent of m. Let $c_m(s) = g_m(s) + p_m(s)$. In this way, we can calculate $c_n(s)$ from the recursion relations; $\mathsf{D}_0(\alpha)$ is obtained from the inverse Laplace transform of $c_n(s)$. In what follows, we expand the relevant generating functions to second order in s and the

results are used to extract the large α (small current) behaviour of the current distribution.

Let us expand the generating functions to second order in s

$$g_m(s) = g_m(0) + A_m s + D_m s^2 + \dots \tag{14a}$$

and

$$p_m(s) = p_m(0) + B_m s + E_m s^2 + \dots . \tag{14b}$$

and upon identifying coefficients of the same order in s, we obtain for the zeroth order

$$g_m(0) = 3g_{m-1}(0) + p_{m-1}(0) \tag{15a}$$

$$p_m(0) = g_{m-1}(0) + 3p_{m-1}(0). \tag{15b}$$

For the first order

$$A_m = 3A_{m-1} + B_{m-1} - 2\alpha_2 g_{m-1}(0) \tag{16a}$$

$$B_m = A_{m-1} + 3B_{m-1} - \alpha_1(n-m)g_{m-1}(0) - (\alpha_1(n-m) + 2\alpha_2)p_{m-1}(0). \tag{16b}$$

For the second order

$$D_m = 3D_{m-1} + E_{m-1} - 2\alpha_2 A_{m-1} + \alpha_2^2 g_{m-1}(0) \tag{17a}$$

$$E_m - D_{m-1} + 3E_{m-1} - \alpha_1(n-m)A_{m-1} - (\alpha_1(n-m) + 2\alpha_2)B_{m-1} + \tfrac{1}{2}\alpha_1^2(n-m)g_{m-1}(0) + (\alpha_2^2 + \tfrac{1}{2}\alpha_1^2(n-m))p_{m-1}(0) \tag{17b}$$

and so on. Note that the first-order coefficients depend on the zeroth-order coefficients while the second-order coefficients depend on the first- as well as the zeroth-order coefficients. Here we have expanded the generating functions to second order in s for simplicity. Higher-order expansions can, in principle, be obtained in essentially the same way, assisted by computer algebra. By using initial conditions, we arrive at $A_0 = B_0 = D_0 = E_0 = 0$. Moreover, let us define $C_m \equiv A_m + B_m$. We find that

$$C_m = 4C_{m-1} - (\alpha_1(n-m) + 2\alpha_2)(g_{m-1}(0) + p_{m-1}(0)). \tag{18}$$

Similarly we define $F_m = D_m + E_m$ and obtain

$$F_m = 4F_{m-1} - (\alpha_1(n-m) + 2\alpha_2)(A_{m-1} + B_{m-1}) + (\alpha_2^2 + \tfrac{1}{2}\alpha_1^2(n-m))(g_{m-1}(0) + p_{m-1}(0)). \tag{19}$$

The general solutions for $g_m(0)$ and $p_m(0)$ are given by

$$g_m(0) = \tfrac{1}{2}(4^m + 2^m) \tag{20a}$$

$$p_m(0) = \tfrac{1}{2}(4^m - 2^m). \tag{20b}$$

Physically $g_m(0)$ and $p_m(0)$ represent, respectively, the number of good and poor conducting bonds at the mth generation. The homogeneous solution for C_m is $C_m = (2a')\,4^m$, while the particular solution should be of the form

$$C_m = (m(c_1 m + c_2) + c_3)4^m.$$

With the initial condition $C_0 = 0$, the general solution is given by

$$C_m = (m(c_1 m + c_2))4^m. \tag{21}$$

Similarly we obtain the second-order coefficient

$$F_m = (d_1 m^4 + d_2 m^3 + d_3 m^2 + d_4 m)4^m. \tag{22}$$

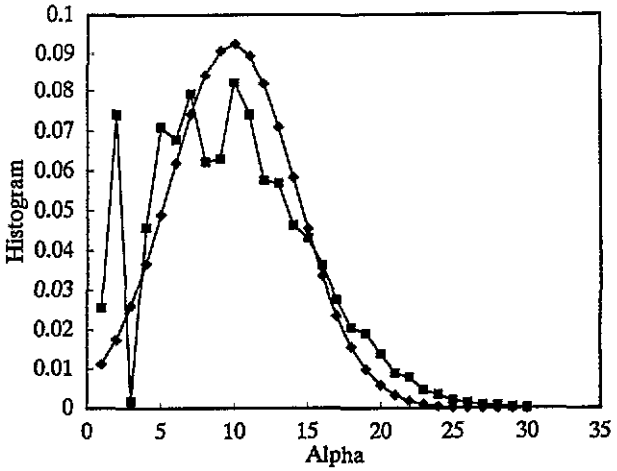

Figure 4. Current distribution in the deterministic percolation model as compared to the Gaussian approximation. The size $L=2^8$ and $h=10^{-6}$.

We are now in ' osition to obtain the mean and the variance of the current distribution. Let us define the moment generating function $c_n(s)=g_n(s)+p_n(s)$ for which $D_0(\alpha)$ is the inverse Laplace transform of $c_n(s)$. If we expand $c_n(s)$ to second order in s, we find

$$c_n(s)=c_n(0)(1-\langle\alpha\rangle s+\tfrac{1}{2}\langle\alpha^2\rangle s^2+\ldots) \tag{23}$$

where $\langle\alpha^m\rangle$ is the mth moment of $D_0(\alpha)$

$$\langle\alpha^m\rangle=\int_0^\infty \alpha^m D_0(\alpha)\,d\alpha \Big/ \int_0^\infty D_0(\alpha)\,d\alpha. \tag{24}$$

The mean and variance of $D_0(\alpha)$ can be identified as

$$\langle\alpha\rangle=-C_n/4^n\approx-(c_1n^2+c_2n) \tag{25}$$

and

$$\langle\alpha^2\rangle-\langle\alpha\rangle^2=2F_n/4^n-(C_n/4^n)^2. \tag{26}$$

It is remarkable to find that the mean of the current distribution varies with n as $-n^2$, which is identical to the scaling form of the minimum current. Due to the fact that $c_1=2d_1$, the highest order term n^4 in the variance $\langle\alpha^2\rangle-\langle\alpha\rangle^2$ is cancelled out so that the variance varies as n^3.

Here we check the Gaussian approximation numerically. For $n=8$, $h_0=10^{-6}$, the analytic calculation gives the $C_n=-9.864$, $F_n=57.955$, and $\langle\alpha^2\rangle-\langle\alpha\rangle^2=18.606$. In figure 4, we plot the histogram and compare with the theoretical Gaussian distribution. Since the histogram for the numerical data is not smooth, we also plot the cumulative histogram in figure 5. There are two reasons for deviation from the Gaussian approximation. First, our expansion only goes to the second order in s, the approximation is only valid for small s and therefore large α. Second, the model includes a small parameter h_0, which is neglected in the present limit, so that the Gaussian approximation is not as good.

5. Local power dissipation

In this section, we use a similar method to obtain the analytic form of the local power distribution. Let us define the power distribution at the kth level of renormalization $P_k(\beta)\,d\beta$ as the number of bonds carrying power with $\beta < -\log p_i < \beta + d\beta$, we also denote $P_k^g(\beta)$ as the power distribution of the good conductors and $P_k^p(\beta)$ that of the poor conductors so that $P_k(\beta) = P_k^g(\beta) + P_k^p(\beta)$. The initial condition at the nth level of renormalization ($k=n$) is $P_n^g(\beta) = \delta_{\alpha,0}$ and $P_n^p(\beta) = 0$. We follow closely the derivation of the current distribution in the preceding section to obtain the local power distribution. Without loss of generality, we again consider the limit $h_n \approx \lambda_0^n h_0 \ll 1$. Again we take $f = \frac{3}{4}$. In the good conducting bonds

$$p_{k1} = \frac{1}{\varphi(0)} p_{k+1} \tag{27a}$$

$$p_{k2} = h_k \frac{1}{\varphi(0)} p_{k+1} \tag{27b}$$

$$p_{k3} = p_{k4} = \frac{1}{4\varphi(0)} p_{k+1} \tag{27c}$$

and in the poor conducting bonds

$$p_{k1} = h_k h j_{k+1} \frac{1}{\varphi(0)} p_{k+1} \tag{28a}$$

$$p_{k2} = h_{k+1} \frac{1}{\varphi(0)} p_{k+1} \tag{28b}$$

$$p_{k3} = p_{k4} = \frac{\lambda_0}{4\varphi(0)} p_{k+1}. \tag{28c}$$

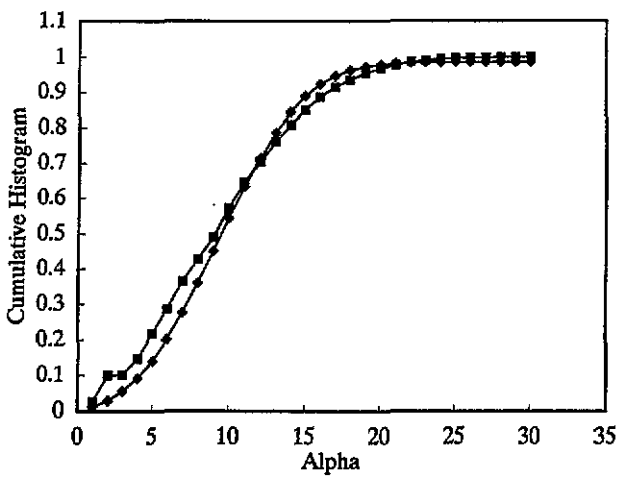

Figure 5. The cumulative histogram for the current distribution in the deterministic percolation model and its Gaussian approximation (same data as in figure 4).

Take the logarithm of (27) and let $\beta = -\log p_k$ and $\beta' = -\log p_{k+1}$, β' being the pre-image of β. Again we define the Laplace transform for the distribution functions

$$y_m(s) = \int_0^\infty \mathrm{P}^g_{n-m}(\beta)\, \mathrm{e}^{-s\beta}\, \mathrm{d}\beta \tag{29a}$$

$$z_m(s) = \int_0^\infty \mathrm{P}^p_{n-m}(\beta)\, \mathrm{e}^{-s\beta}\, \mathrm{d}\beta \tag{29b}$$

at the mth generation with initial conditions $y_0(s) = 1$ and $z_0(s) = 0$. We obtain the following recursion relations

$$y_m(s) = (\mathrm{e}^{-s\beta_1} + 2\mathrm{e}^{-s\beta_3}) y_{m-1}(s) + \mathrm{e}^{-s\beta_5(n-m)} z_{m-1}(s) \tag{30a}$$

$$z_m(s) = \mathrm{e}^{-s\beta_2(n-m)} y_{m-1}(s) + (\mathrm{e}^{-s\beta_4(n-m)} + 2\,\mathrm{e}^{-s\beta_6}) z_{m-1}(s) \tag{30b}$$

where $\beta_1, \ldots, \beta_6$ are parameters. We define $f_m(s) = y_m(s) + z_m(s)$ which is the moment generating function of $\mathrm{P}_0(\beta)$ which is in turn the inverse Laplace transform of $f_n(s)$. As in the preceding section, we expand the generating functions and the coefficients to second order in s. Let

$$y_m(s) = y_m(0) + G_m s + M_m s^2 + \ldots \tag{31a}$$

$$z_m(s) = z_m(0) + H_m s + N_m s^2 + \ldots . \tag{31b}$$

The initial conditions are $y_0(s) = 1$ and $z_0(s) = 0$ and thus $G_0 = H_0 = M_0 = N_0 = 0$. The general solutions for $y_m(0)$ and $z_m(0)$ are the same as those for $g_m(s)$ and $p_m(s)$ respectively while the general solution of S_m is given by

$$S_m = (m(s_1 m + s_2))4^m. \tag{32}$$

The general solution of T_m should be of the form

$$T_m = (t_1 m^4 + t_2 m^3 + t_3 m^2 + t_4 m)4^m. \tag{33}$$

Similarly the mean and the variance of the power distribution is given by the first two moments of the moment generating function $f_n(s) = y_n(s) + z_n(s)$

$$f_n(s) = f_n(0)\,(1 - \langle\beta\rangle s + \tfrac{1}{2}\langle\beta^2\rangle s^2 + \ldots) \tag{34}$$

where $\langle\beta^m\rangle$ is the mth moment of $\mathrm{P}_0(\beta)$

$$\langle\beta^m\rangle = \frac{\displaystyle\int_0^\infty \beta^m \mathrm{P}_0(\beta)\, \mathrm{d}\beta}{\displaystyle\int_0^\infty \mathrm{P}_0(\beta)\, \mathrm{d}\beta}. \tag{35}$$

We identify the mean and variance of $\mathrm{P}_0(\beta)$

$$\langle\beta\rangle = -S_n/4^n \approx -(s_1 n^2 + s_2 n) \tag{36}$$

and

$$\langle\beta^2\rangle - \langle\beta\rangle^2 = 2T_n/4^n - (S_n/4^n)^2. \tag{37}$$

We find that the mean varies with n as $-n^2$, and the variance as n^3, a dependence similar to that of the current distribution. We also check the Gaussian approximation in figure 6 and figure 7 for $n = 8$, $h_0 \approx 10^{-6}$ where the analytic calculation gives $S_n = -19.229$, $T_n = 218.07$, and $\langle\beta^2\rangle - \langle\beta\rangle^2 = 66.399$.

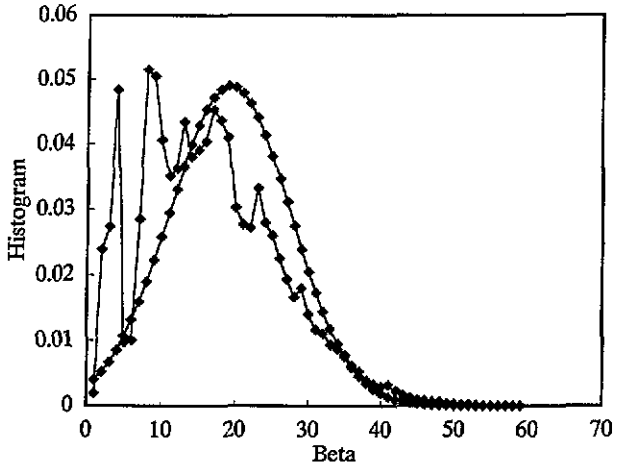

Figure 6. Power distribution in the deterministic percolation model as compared to the Gaussian approximation. The size $L = 2^8$ and $h = 10^{-6}$.

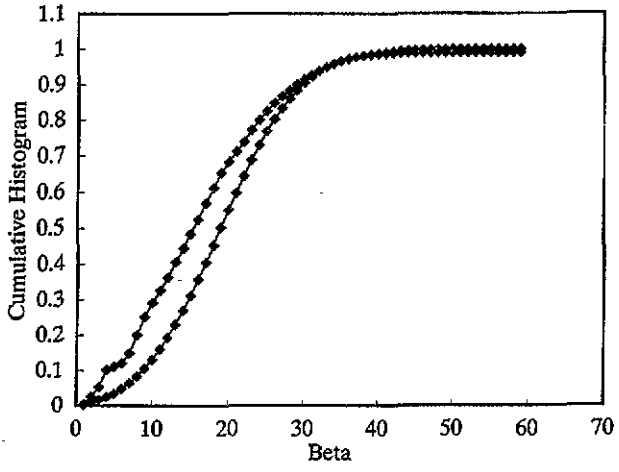

Figure 7. The cumulative histogram for the power distribution in the deterministic percolation model and its Gaussian approximation (same data as in figure 6).

6. Discussion and conclusion

First of all, let us study the generality of the results. We have performed similar calculations in the two-component diamond lattice [13], which is the exact dual lattice of DPM. We also performed numerical simulations on two-dimensional random resistor networks [6]. To this end, we should remark that the minimum current is extremely difficult to determine accurately in numerical simulations. We instead determine the most probable current, which was shown to scale in the same way as the minimum current does. We obtained the same $\exp[-c(\ln h)^2]$ behaviour. It would be interesting to perform extensive numerical simulations especially in three dimensions to check the analytic results.

Secondly, we develop the multifractal aspect of the model, i.e. we compute the left side of the $f(\alpha)$ spectrum. We consider the partition function

$$\Sigma_i I_i^{2q} \approx L^{-\tau(q)}$$

according to multifractal analysis [10]. For $h=1$, we find $\tau(q)=2(1-q)$, which indicates a constant-gap scaling. The $f(\alpha)$ spectrum is a single point at $\alpha=f=2$. For $h=0$, we recover the deterministic fractal lattice of [12]. When $h\to 0$, the maximum current $I_{\max}\to 1$. For $q\geqslant 0$ and for sufficiently large size $L=2^n$, the partition function scales as

$$\Sigma_i I_i^{2q} \approx (1+2^{-(2q-1)})^n.$$

We obtain $\tau(q)=\ln[1+2^{-(2q-1)}]/\ln 2$. Tremblay *et al* [14] did Monte Carlo simulations for integral values of $q=1$, 2 and 3 only. We find $\tau(1)=-0.585$, $\tau(2)=-0.167$ and $\tau(3)=-0.044$, in qualitative agreements with the results $\tau(1)=-0.98$, $\tau(2)=-0.82$ and $\tau(3)=-0.77$ of Tremblay *et al* [14]; in particular the inequality $|\tau(q)|>|\tau(q+1)|$ is strictly obeyed. One should not be surprised too much by such a discrepancy because deterministic fractral models can only capture qualitatively the scaling behaviour of percolation clusters.

It would be nice to do some experiments on random resistor–capacitor networks [12] in which the frequency-dependent admittance ($G\approx i\omega C$) of capacitors plays the same role as the small parameter h of the problem. Thus by varying the frequency ω of the external alternating current, one might mimic the crossover behaviours described in this work.

In conclusion, we present an analytical solution of the current distribution in the deterministic percolation model which consists of two types of conductance, parameterized by the ratio h of poor to good conductance. Due to the iterative nature of the model, we are able to find exact recursion relations for the current distribution. For extremely small h such that $hL^{\phi}\ll 1$, where L is the size of the lattice and ϕ the crossover exponent, the current distribution is well approximated by a Gaussian with the mean varying with size as $(\log L)^2$ while the variance as $(\log L)^3$. We find that $D(\alpha)\,d\alpha \approx \exp(-A[\alpha-B(\log L)^2]/(\log L)^3)$, where $D(\alpha)\,d\alpha$ is the number of currents with $\alpha<-\log I_i<\alpha+d\alpha$; I_i is the current in bond i and A, B are constants. In the opposite limit $hL^{\phi}\gg 1$, the distribution reduces to the trivial form of a one-component percolating lattice. As a result, both the most probable current and the minimum current scale with L as $\exp[-\text{constant}\,(\log L)^2]$. We also examine the local power distribution and find similar scaling behaviour.

Acknowledgment

KWY acknowledges the support from the Direct Grant under Project Number 220–600–240 from the Chinese University.

References

[1] Rammal R, Tannous C, Breton P and Tremblay A-M S 1985 *Phys. Rev. Lett.* **54** 1718
[2] de Arcangelis L, Redner S and Coniglio A 1985 *Phys. Rev.* B **31**, 4725; 1986 *Phys. Rev.* B **34** 4656
[3] de Arcangelis L and Coniglio A 1987 *J. Stat. Phys.* **48** 935
[4] Tremblay R R, Albinet G and Tremblay A-M S 1991 *Phys. Rev.* B **43** 11546
Tremblay A-M S, Fourcade B and Breton P 1989 *Physica* **157A** 89

[5] Kolek A 1992 *Phys. Rev.* B **45** 205
[6] Tong P Y and Yu K W 1993 *J. Phys. A: Math. Gen.* **26** L119
Yu K W and Tong P Y 1992 *Phys. Rev.* B **46** 12137
[7] Blumenfeld R and Aharony A 1989 *Phys. Rev. Lett.* **62** 2977
Kahng B and Lee J 1990 *J. Phys. A: Math. Gen.* **23** L747
Stanley H E, Bunde A, Havlin S, Lee J, Roman E and Schwarzer S 1990 *Physica* **168A** 23
Mandelbrot B B, Evertsz C J G and Hayakawa Y 1990 *Phys. Rev.* A **42** 4528
[8] Frisch U and Parisi G 1985 *Turbulence and Predictability of Geophysical Flows and Climate Dynamics, Proc. Int. School of Physics 'Enrico Fermi'* ed M Ghil, R Benzi, and G Parisi (New York: North-Holland) p 84
[9] Halsey T C, Jensen M H, Kadanoff L P, Procaccia I, and Shraiman B I 1986 *Phys. Rev.* A **33** 1141
[10] Lee J, Havlin S, and Stanley H E 1992 *Phys. Rev.* A **45** 1035
[11] Kirkpatrick S 1978 *Proc. ETOPM1 Conf., AIP Conf. Proc.* **40** 79
Kirkpatrick S 1979 *Proc. Les Houches Summer School on Ill-Condensed Matter* ed R Balian, R Maynard and G Toulouse (Amsterdam: North-Holland) p 321
[12] Clerc J P, Giraud G, Laugier J M and Luck J M 1990 *Adv. Phys.* **39** 191
[13] Berker A N and Ostlund S 1979 *J. Phys. C: Solid State Phys.* **12** 4961
Yu K W and Tong P Y 1992 *Phys. Rev.* B **46** 11487
[14] Tremblay R R, Albinet G and Tremblay A-M S 1992 *Phys. Rev.* B **45** 755